Accepted Manuscript

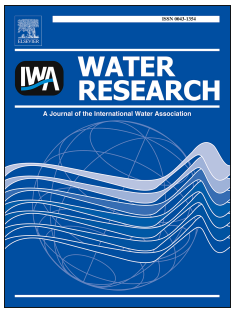

Sulfate removal and sulfur transformation in constructed wetlands: The roles of filling material and plant biomass

Yi Chen, Yue Wen, Qi Zhou, Jingang Huang, Jan Vymazal, Peter Kuschk

PII: S0043-1354(16)30505-X

DOI: 10.1016/j.watres.2016.07.001

Reference: WR 12196

To appear in: *Water Research*

Received Date: 29 April 2016

Revised Date: 1 July 2016

Accepted Date: 2 July 2016

Please cite this article as: Chen, Y., Wen, Y., Zhou, Q., Huang, J., Vymazal, J., Kuschk, P., Sulfate removal and sulfur transformation in constructed wetlands: The roles of filling material and plant biomass, *Water Research* (2016), doi: 10.1016/j.watres.2016.07.001.

This is a PDF file of an unedited manuscript that has been accepted for publication. As a service to our customers we are providing this early version of the manuscript. The manuscript will undergo copyediting, typesetting, and review of the resulting proof before it is published in its final form. Please note that during the production process errors may be discovered which could affect the content, and all legal disclaimers that apply to the journal pertain.

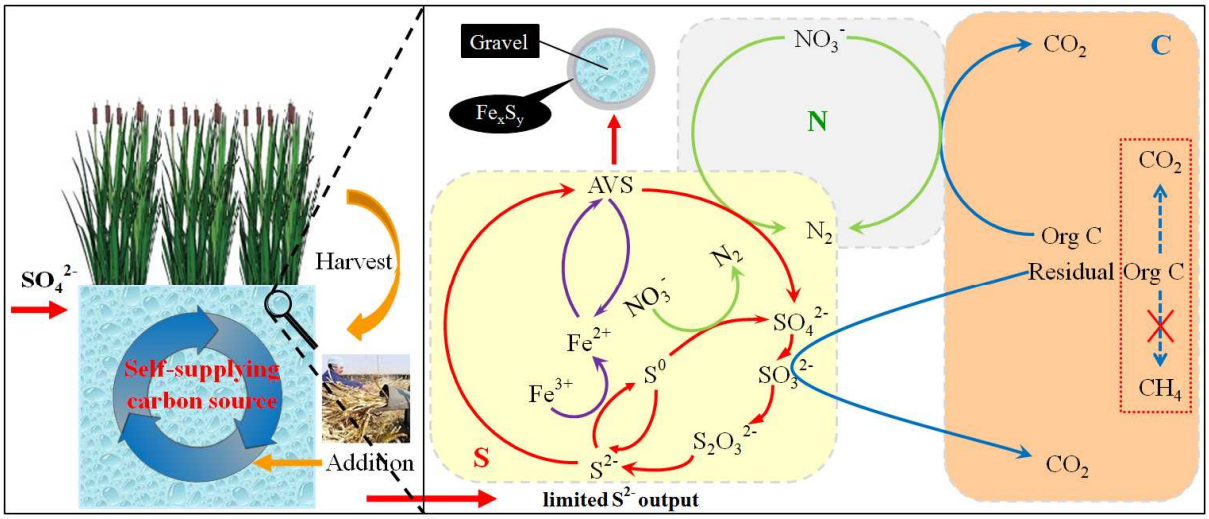

ACCEPTED MANUSCRIPT

ACCEPTED MANUSCRIPT

Sulfate removal and sulfur transformation in constructed wetlands: The roles of filling material and plant biomass

Yi Chen[a,b], Yue Wen[a] *, Qi Zhou[a], Jingang Huang[c], Jan Vymazal[b], Peter Kuschk[d]

[a]*Key Laboratory of Yangtze Water Environment of Ministry of the State Education, College of Environmental Science and Engineering, Tongji University, Shanghai 200092, P.R. China*

[b] *Department of Applied Ecology, Faculty of Environmental Sciences, Czech University of Life Sciences Prague,16521, Czech Republic*

[c]*Institute of Environmental Science and Engineering, Hangzhou Dianzi University, Hangzhou 310018, PR China.*

[d] *Department of Environmental Biotechnology, Helmholtz Centre for Environmental Research —UFZ, Permoserstr.15, 04318 Leipzig, Germany.*

* Corresponding author. Present address: Room 301, Mingjing Building, School of Environmental Science and Engineering, Tongji University, Shanghai 200092, P.R. China. Tel.: 86-21-65982697; fax: 86-21-65982697.

E-mail address: *weny@tongji.edu.cn* (Y. Wen).

Abstract

Sulfate in effluent is a challenging issue for wastewater reuse around the world. In this study, sulfur (S) removal and transformation in five batch constructed wetlands (CWs) treating secondary effluent were investigated. The results showed that the presence of the plant cattail (*Typha latifolia*) had little effect on sulfate removal, while the carbon-rich litter it generated greatly improved sulfate removal, but with limited sulfide accumulation in the pore-water. After sulfate removal, most of the S was deposited with the valence states S (-II) and S (0) on the iron-rich gravel surface, and acid volatile sulfide was the main S sink in the litter-added CWs. High-throughput pyrosequencing revealed that sulfate-reducing bacteria (i.e. *Desulfobacter*) and sulfide-oxidizing bacteria (i.e. *Thiobacillus*) were dominant in the litter-added CWs, which led to a sustainable S cycle between sulfate and sulfide. Overall, this study suggests that recycling plant litter and iron-rich filling material in CWs gives an opportunity to utilize the S in the wastewater as both an electron acceptor for sulfate reduction and as an electron donor for nitrate reduction coupled with sulfide oxidation. This leads to the simultaneous removal of sulfate, nitrate, and organics without discharging toxic sulfide into the receiving water body.

Keywords

Constructed wetlands; Bacterial sulfate reduction; Sulfur oxidation; Denitrification; Plant litter

ACCEPTED MANUSCRIPT

1 Introduction

Sulfate is a common contaminant of wastewater, and is not usually considered a health concern, but it can, under some circumstances, cause diarrhea. However, sulfate reduction may produce hydrogen sulfide (H_2S) and organic sulfur (S) compounds, which normally cause aesthetic problems (taste, color and/or odor) in the wastewater and the effluent-dominated river. Moreover, H_2S can cause serious corrosion to water pipes during the transportation of reused water and/or phytotoxicity to plants during irrigation (EPA, 2004). Therefore, the removal of sulfate in the effluent from wastewater treatment plants (WWTP) with minimum H_2S accumulation is of great importance to wastewater reuse around the world.

Constructed wetlands (CWs) are widely used as a tertiary treatment to polish the WWTP effluent for wastewater reuse due to their low implementation costs, simple operation, and efficient removal of effluent contaminants (Greenway, 2004; Jasper et al., 2014). CWs act as an eco-buffer zone between the WWTP and receiving waters, and could become promising artificial ecosystems for odor control in effluent-dominated rivers if the majority of the S could be immobilized or dissipated in CWs beds. Sulfur transformation in CWs has become increasingly important in recent years due to the high S reduction and oxidation activities shown in wetlands (Baldwin and Mitchell, 2012; Wu et al., 2013). In subsurface flow constructed wetlands (SSF CWs), the relatively low redox condition provides a high thermodynamic potential for sulfate reduction. However, the amount of internal carbon from the rhizosphere and external

carbon from secondary effluent are not enough to drive significant sulfate reductions in CWs (Stein et al., 2007). Plant litter is one of the most abundant carbon sinks in wetlands (500-2000 g C $m^{-2}yr^{-1}$) (Hume et al., 2002). While, the structure of SSF CWs prevents aboveground plant litter from reaching the subsurface water and inhibits the carbon release from plant litter. Therefore, recycling the carbon in plant litter could be a low cost and sustainable way to enhance sulfate reduction in CWs. Chen et al. (2014) showed that plant litter greatly stimulated sulfate reduction in CWs through the on-site production of carbon sources such as carbohydrate and volatile fatty acids. However, as far as can be ascertained, there have not been any studies on the effect of plant litter on S transformation in CWs treating secondary effluent.

Sulfide is considered to be the main product of sulfate reduction, and can severely inhibit ammonium/carbon removal and plant photosynthesis, which decreases the treatment efficiency of CWs. Sulfide detoxification can be achieved when CWs are supplied/filled with metal-enriched substrates, because sulfide can precipitate along with heavy metals (i.e. iron, zinc) (Stein et al., 2007; Wu et al., 2012). Wiessner et al. (2010) calculated that nearly half the sulfate-S was immobilized inside CWs. However, the amount and speciation of the immobilized S (solid-phase) is often unknown. Acid volatile sulfide (AVS) is considered to be the main component in the solid-phase S, and it is a complex and variable component that includes diverse reduced S forms (e.g. FeS, Fe_3S_4, and FeS_2) (Rickard and Morse, 2005). At present, AVS detection relies on the

application of acid-based extraction methods, which are relatively efficient, but do not detect 100% of the AVS since not all of the Fe_xS_y can be fully extracted. X-ray photoelectron spectros-copy (XPS) has emerged as an element-sensitive technique for describing the speciation and distribution of S at the microscale in recent years (Sun et al., 2009). Despite the wide use of acid-based AVS extraction and S speciation identification by XPS (Baldwin and Mitchell, 2012; Johnston et al., 2014), very few studies have investigated the solid-phase S in the filling material of CWs. Therefore, there has not been complete elucidation of the S species distribution and related S transformations in CWs.

Apart from the precipitation of sulfide with metals, oxidation is another effective method of avoiding sulfide accumulation. Oxygen released from plant roots and the atmosphere oxidizes harmful sulfide to harmless forms (e.g. elemental S and sulfate) in CWs (Faulwetter et al., 2009). Previous studies have suggested that 41%–90% of the reduced S was re-oxidized by root-mediated oxygen in planted wetlands (Wiessner et al., 2010; Wu et al., 2011). Wu et al. (2011) further demonstrated the multiple S transformations (i.e. sulfide re-oxidation) in CWs using the ^{34}S isotope approach. Apart from oxygen, nitrate in the influent can also easily drive sulfide and elemental S oxidation to sulfate in the organic-rich wetlands (Krishnakumar and Manilal, 1999; Londry and Suflita, 1999). Chemical and microbial oxidation are the main sulfide oxidation processes in CWs (Wu et al., 2013). Bacterial sulfur oxidation is mainly

104 driven by S oxidizing bacteria (SOB), and sulfide is oxidized to sulfur (or sulfate) using
105 oxygen or nitrate as electron acceptors (Faulwetter et al., 2009). At present, information
106 on the SOB community in CWs is incomplete due to the inefficient detection of species
107 that are present at low levels (Hallberg and Johnson, 2005; Nicomrat et al., 2006).
108 Therefore, a sensitive and comprehensive detection method for S-related bacteria based
109 on next-generation sequencing is urgently needed to improve understanding of the
110 mechanism underlying microbial S oxidation in CWs.

111 In this study, S transformation was characterized in five iron-rich media containing
112 CWs with or without cattail (*Typha latifolia*) and externally added carbon sources. The
113 objectives were to (1) study the effects of plants and plant litter as carbon sources on
114 sulfate removal, sulfide accumulation, and intermediate-S formation. (2) quantify the
115 solid AVS and the multi-valence distribution of S in the iron-rich gravel; (3) quantify S
116 species distribution and elucidate S transformation; and (4) characterize the structures of
117 SRB/SOB communities in CWs.

118 **2 Materials and Methods**

119 **2.1 Design and operation of the SSF CW**

120 Five sequencing batch SSF CW microcosms, each with a bulk volume of 0.045 m^3
121 (length: 0.3 m, width: 0.3 m, height: 0.5 m) and a pore volume of 12 L, were set up in
122 this study. Five systems: an unplanted control (W0), two litter-added microcosms (W1:
123 100g; W2: 200g), a planted microcosm (W3: 22 plants m^{-2}) and a planted plus litter

124 added microcosm (W4: 100g litter, 22 plants m^{-2}), were established. All the microcosms
125 were filled with iron-rich gravel (ϕ8–13 mm, porosity = 0.4, iron content 4.7%, w/w)
126 up to a height of 40 cm. The water level was adjusted to be 5 cm below the gravel bed
127 surface. Two (W3 and W4) CWs were planted with cattail (*Typha latifolia*). The wetland
128 microcosms have been located in an air-conditioned greenhouse at a temperature of 25 ±
129 1 ^{o}C since 2005. Prior to the start of the experiment, the five microcosms were fed, in
130 batches, with a modified secondary effluent for 6 months pre-incubation in order to
131 establish the plant shoots and microorganisms. Then, cattail litter (1~1.5 cm lengths)
132 was added to the W1, W2, and W4 microcosms as the carbon source to drive sulfate
133 reduction. The cattail litter was homogeneously mixed with gravel, and the mixed
134 media were compacted with a tamping rod at 5 cm increments during loading and filled
135 the microcosms to a height of 40 cm.

136 **2.2 Batch experiment**

137 The batch experiment began after a 6 month pre-incubation. The wetland
138 microcosms were fed with the secondary effluent from a neighboring WWTP, and the
139 characteristics of the wetland influent were seen in Table S1. Influent was introduced
140 into the microcosm from the top and gravity drained from the bottom. The microcosm
141 was operated in batch mode with five days for each batch (HRT = 5 d). Feeding,
142 reaction and draining was designed as illustrated in Figure 1. Briefly, each batch started
143 with a feeding stage (1 h), followed by a reaction stage (118 h), and terminated with a

144 draining stage (1 h). All the treatments (W0–W4) were triplicated and the duration of
145 the batch experiment was 100 d, which included 20 batches. Water samples were taken
146 from each microcosm and each batch. A 100 mL syringe was used to collect water
147 samples at 5, 20, and 30 cm depths from the central sampling pipe. Only water samples
148 taken from 20 cm depth were reported because no vertical gradients in the water
149 chemistry were observed in the preliminary experiment and in previous experiments
150 with the same microcosms (Wen et al., 2010).

151 **2.3 S-based autotrophic denitrification kinetic tests**

152 The autotrophic denitrification kinetic tests were carried out according to Chen et
153 al. (2014b). Briefly, 1000 g of gravel was taken from W0–W4 before batch 20 and
154 respectively transferred to 1 L serum bottles (S0–S4). After a 10 d pre-incubation period
155 (removal of the original nitrate, sulfate, and endogenous organic matters inside the cell),
156 nitrate (10 mg L^{-1} NO_3^--N) was added to the serum bottles, which were then incubated
157 in an anaerobic environment (25 ^oC) for five days. Nitrate and sulfate concentrations
158 were measured every 12 h. There was no organic carbon in the feeding water, so nitrate
159 loss in the serum bottles could be mainly attributed to autotrophic denitrification.

160 **2.4 Aqueous-phase methods**

161 Five 50 mL water samples, withdrawn at the appropriate time intervals, were
162 membrane-filtered (0.22 μm) and immediately analyzed for dissolved sulfide. Zinc
163 chloride solution was then added (prior to further analysis for other chemical

164 constituents) to the filtered samples in order to eliminate any soluble sulfide by
165 precipitating it as zinc sulfide. Sulfate, sulfite, thiosulfate, and nitrate were detected
166 using a DX ICS-3000 ion chromatography unit (Dionex Corporation, CA, USA)
167 equipped with a conductivity detector and a self-regenerating suppressor
168 ASRS-ULTRA II 4-mm (129 mA). Elemental sulfur was detected by HPLC (Agilent
169 1200, Agilent Technologies, CA, USA) using a Li-Chrospher 100, RP 18 column
170 equipped with an UV detector at 263 nm. Dissolved sulfide and chemical oxygen
171 demand (COD) were analyzed using standard methods (APHA, 1998). The Eh was
172 measured using a portable mV/ pH /temperature meter (HACH, sensION1, USA) fitted
173 with an Ag/AgCl Eh electrode. The details of the S compound analyses were reported in
174 a previous study (Chen et al., 2014a).

175 **2.5 Solid-phase methods**

176 For the AVS-S analysis, 64 gravel samples were collected from four different layers
177 (10, 20, 30, and 40 cm) after the experiment. Then, 500 g of composited gravel was
178 extracted with 1 M HCl, and the produced H_2S was trapped in 0.05 M Zn acetate and
179 quantified by iodometric titration. XPS experiments were carried out on an RBD
180 upgraded PHI-5000C ESCA system (Perkin–Elmer) with Al Kα radiation (hν = 1486.6
181 eV). Curve fitting of the carbon C1s peaks were achieved by fitting them to Gaussian
182 curves using RBD AugerScan 3.21 software. A scanning electron microscope (Philips,
183 XL30) and an energy dispersive spectrometer (Link 300) were used to observe the

ACCEPTED MANUSCRIPT

surface morphology and analyze the elemental distribution on the surface of the gravel.

2.6 DNA extraction

After batch 20 (100d), approximately 200g of gravel and litter were collected from the top (5 cm), middle (20 cm), and bottom (40 cm) sections of the wetland microcosms. The three samples were combined for DNA extraction. Before DNA extraction, the gravel/litter samples were vigorously shaken at 225 rpm for 3 h in sterile glass bottles in order to suspend any attached biofilm in the liquid solution. The precipitate was collected in bottles for further analysis after they had been centrifuged twice at 5000g for 20 min. Total genomic DNA was extracted from the gravels and litters using an E.Z.N.A. ® Soil DNA Kit (OMEGA bio-tek). The quantity and quality of the extracted DNA were checked by measuring its absorbance at 260 and 280 nm using a UNICO-2100 UV/VIS spectrophotometer.

2.7 High-throughput 16S rRNA gene sequencing and analysis

High-throughput 454 GS-FLX pyrosequencing of the 16S rRNA gene was conducted according to standard protocols (Margulies et al., 2005). A BLAST search for taxonomic classification down to the phylum, class and genus levels was then undertaken using MOTHUR and the SILVA 106 database with a set confidence threshold of 80%. The pyrosequencing and analysis details were reported in a previous study (Chen et al., 2015).

204 **2.8 Mass balance calculations**

205 In this study, total sulfur was calculated by summing up all the determined sulfur
206 compounds (SO_4^{2-}, S^0, S^{2-}, $S_2O_3^{2-}$ and AVS) and undetermined sulfur compounds (other
207 S). Assuming that the mass of total sulfur was constant after CW treatment, the
208 following equation can be obtained:

$$\Delta m_{\text{total S}} = \Delta m_{SO_4^{2-}} + \Delta m_{S^0} + \Delta m_{S^{2-}} + \Delta m_{S_2O_3^{2-}} + \Delta m_{\text{AVS}} + \Delta m_{\text{other S}} = 0 \quad (1)$$

$$\Delta m_{\text{other S}} = -\Delta m_{SO_4^{2-}} - \Delta m_{S^0} - \Delta m_{S^{2-}} - \Delta m_{S_2O_3^{2-}} - \Delta m_{\text{AVS}} \quad (2)$$

209 The mass removal of the determined sulfur compounds is obtained from the following
210 equation:

$$\Delta m_{SO_4^{2-}} = \sum_{i=1}^{n} (C_{i(in)SO_4^{2-}} \times V_{i(in)} - C_{i(out)SO_4^{2-}} \times V_{i(out)}) \quad (3)$$

$$\Delta m_{S^0} = \sum_{i=1}^{n} (C_{i(in)S^0} \times V_{i(in)} - C_{i(out)S^0} \times V_{i(out)}) \quad (4)$$

$$\Delta m_{S^{2-}} = \sum_{i=1}^{n} (C_{i(in)S^{2-}} \times V_{i(in)} - C_{i(out)S^{2-}} \times V_{i(out)}) \quad (5)$$

$$\Delta m_{S_2O_3^{2-}} = \sum_{i=1}^{n} (C_{i(in)S_2O_3^{2-}} \times V_{i(in)} - C_{i(out)S_2O_3^{2-}} \times V_{i(out)}) \quad (6)$$

$$\Delta m_{\text{AVS}} = m_{AVS-ini} - m_{AVS-end} \quad (7)$$

211 where $\Delta m_{SO_4^{2-}}$, Δm_{S^0}, $\Delta m_{S^{2-}}$, $\Delta m_{S_2O_3^{2-}}$ are respectively the mass removal of sulfate,
212 elemental sulfur, sulfide and thiosulfate after CW treatment (mg); Δm_{AVS} is the mass
213 change of acid volatile sulfide in CWs after the batch experiment (mg); $\Delta m_{AVS-ini}$ and

ACCEPTED MANUSCRIPT

214 $\Delta m_{AVS-end}$ are the mass of acid volatile sulfide in gravel before and after the batch
215 experiment, respectively (mg); Δm_{otherS} is the mass removal of undetermined sulfur
216 (mg); i is the number of batch in sequence (i=1,2,3...20); n is the total number of
217 batches; $C_{i(in)}$ and $C_{i(out)}$ are the concentrations of determined sulfur compounds in
218 the influent and effluent of batch i, respectively ($mg \cdot L^{-1}$); $V_{i(in)}$ and $V_{i(out)}$ are the
219 volume of pore water in the influent and effluent of batch i, respectively (L).

220 **3. Results**

221 The experiment was divided into three stages based on the sulfate removal
222 characteristics: an initial stage (days 1–30, batches 1–6), a middle stage (days 31–70,
223 batches 7–14), and a terminal stage (days 71–100, batches 15–20). The sulfate removal
224 kinetics followed a similar pattern at each stage. Therefore, batches 4 (B4), 12 (B12),
225 and 20 (B 20) were chosen as typical batches that represented the three stages,
226 respectively.

227 **3.1 Sulfur compound dynamics in CW pore water**

228 ***3.1.1 Sulfate***

229 Figure 2 shows that there were no significant sulfate decreases in the control (W0)
230 and planted only systems (W3). This suggested that both the influent organic matter and
231 plant root exudates have little effect on sulfate removal. In contrast, significant sulfate
232 removals were observed in the litter-added microcosms, which indicated that cattail
233 litter could act as carbon sources for sulfate reduction. Complete sulfate removal was

ACCEPTED MANUSCRIPT

234 only achieved in the W2 microcosm during the initial stage, and sulfate removal rates
235 gradually decreased over time due to the reduction in organic carbon provided by cattail
236 litter. A previous study showed that the different sulfate removal behaviors were mainly
237 due to the litter decomposition rates and carbon supply in the CWs (Chen et al., 2014a).
238 Figure 2 also shows that sulfate concentrations increased in the litter-added CWs during
239 initial period of each batch, but then decreased in the later stages. This indicated that
240 sulfur oxidation of the deposited S compounds in the bed may also occur in litter-added
241 CWs.

242 ***3.1.2 Sulfide***

243 Sulfide is the final product during sulfate reduction, and its production is
244 encouraged in order to precipitate metals such as Cu, Pb, Cd and Zn (Stein et al., 2007).
245 In this study, the sulfide concentrations were small in the microcosms without litter,
246 which was probably due to the lack of carbon sources to drive sulfate reduction. In
247 contrast, sulfide was detected in all the litter-added microcosms, and its concentration
248 decreased between the initial and the terminal stages. In this study, the sulfide
249 concentrations were always below 1 mg L^{-1} in the litter-added microcosms, which was
250 much lower than the theoretical production through sulfate reduction. The efficient
251 sulfate removal with little sulfide accumulation in the litter-added microcosms was
252 probably due to hydrogen sulfide emissions, metal sulfide precipitation, and sulfide
253 re-oxidation (Wu et al., 2013).

ACCEPTED MANUSCRIPT

3.1.3 Intermediate S compounds

Elemental S, thiosulfate and sulfite are the common intermediate compounds in the wetland S cycle (Wiessner et al., 2010). These intermediate S compounds are not stable in wetlands and can be oxidized or reduced via different pathways (Wu et al., 2013). In this study, the elemental S was only detected in the pore water of the litter-added microcosms, and the maximum concentration increased from 0.9 mg L^{-1} at the initial stage to 4.4 mg L^{-1} at the terminal stage. The increased elemental S over time was probably caused by the gradual accumulation of reduced S in the microcosms, and it can be oxidized to elemental S once oxygen or nitrate is available. Figure 3 shows that thiosulfate was only detected in the litter-added microcosms during the initial and middle stages, and the highest concentration was observed in the W2 microcosm. This suggested that carbon sources played an important role in the production of thiosulfate. In this study, sulfite was not detected in all the microcosms, which indicated that the sulfite reduction rate outpaced its production rate.

3.2 Solid reduced S in the gravel

3.2.1 Acid-volatile sulfides (*AVS*)

AVS are sedimentary S pools that can generate gaseous H_2S following the addition of acid. Both S in the soluble phase (HS^-, H_2S and $FeHS^+$) and S in the solid phase (FeS, FeS_2 and Fe_3S_4) could be considered as sources of AVS (Rickard and Morse, 2005). In this study, solid reduced S was the main component of AVS due to the extraction of S in

274 the gravel. As shown in Figure S1, the highest AVS accumulation (1806 mg) was
275 observed in the W2 microcosm gravel, which indicated that added carbon sources from
276 plant litters increased AVS accumulation in wetlands. Furthermore, there was no
277 significant difference in AVS accumulation between the W1 (824 mg) and W4 (859 mg)
278 microcosms, suggesting that adding plants may not significantly affect AVS
279 accumulation in wetlands. According to the mass calculation, 23.5, 66.3 and 15.8 mg
280 soluble sulfide were detected in the W1, W2 and W4 microcosms, respectively, which
281 were much lower than their individual AVS accumulations. This suggested that solid
282 AVS sources other than soluble sulfide were the main sink for the reduced S in wetlands
283 with added litter. The S valence was further analyzed using XPS in order to determine
284 the diverse reduced and oxidized S forms in the wetland gravel.

285 ***3.2.2 Sulfur valences***

286 One broad characteristic peak was observed on the gravel XPS S2*p* spectra (Figure
287 4). The broad peak located between 158 and 168 eV was divided into one doublet and
288 one singlet (Sun et al., 2009): the S2$p_{3/2\text{-}1/2}$ doublet at 161.5 and 162.6 eV were
289 attributed to S (-II), and the S2$p_{3/2}$ singlet at 163.6 eV was assigned to S (0). Figure 4
290 also shows that both the S (-II) and S (0) characteristic peaks were observed in the
291 litter-added microcosms, which indicated that S reduction and oxidation coexisted in
292 wetlands. Furthermore, the relative peak area ratios for S (0):S (-II) were 0.21:1.00,
293 0.36:1.00, and 0.22:1.00 in the W1, W2, and W4 microcosms, respectively. The larger

ACCEPTED MANUSCRIPT

294 relative peak areas for S (-II) compared to of S (0) indicated that S (-II) was the main S
295 valence in the gravel and that there was limited S transformation from a lower valence
296 to a higher one. The electron binding energies (161.5 and 162.6 eV) suggested that FeS
297 and FeS_2 could be the main components of the solid AVS in this study (Crist, 1999). The
298 energy-dispersive X-ray spectroscopy (EDS) analysis also showed that Fe was present
299 at high levels (4.66%), and there was no Cu, Pb, Cd, Zn, Ni, or Mn in the initial gravel
300 (Figure S3), which indicated that Fe-S precipitation had a dominant role in the
301 production of solid AVS.

302 **3.3 Sulfur species distribution**

303 After the experiment, the S species distribution was calculated based on the S mass
304 balance (Section 2.8). There was very little sulfate removal in the control (W0) and
305 planted microcosms (W3). Therefore, S species distribution data were only available for
306 the litter-added microcosms (W1, W2, and W4). Figure 5 shows that the highest total
307 sulfate removal was observed in W2 (2345.6 mg S), followed by W4 (1312.9 mg S) and
308 W1 (1148.8 mg S). Furthermore, 65.4%–77.0% of the sulfate-S was transformed into
309 AVS and immobilized in the gravel. As an intermediate product of sulfide oxidation, S^0
310 accounted for 4.5%–7.5% of the sulfate removal in the litter-added microcosms. In
311 addition to solid AVS, sulfide, elemental S and thiosulfate, there were some unidentified
312 S compounds and they contributed 10.2%–25.9% to the total amount of sulfate-S that
313 was transformed. These unaccounted S may mainly originate from the intermediate

314 products during the S cycling (i.e. S_x^{2-}, $S_4O_6^{2-}$) or the organic sulfides rather than
315 gaseous sulfide (H_2S) (lower than detection limit in this study) (Isamu et al., 1999).

316 **3.4 Sulfur-driven autotrophic denitrification**

317 In this study, the accumulation of AVS/S^0 in the litter-added CWs and the production
318 of nitrate in the secondary effluent provided an opportunity to connect sulfur oxidation
319 to nitrate reduction (Eq. 1). In the batch experiment, the production of sulfate (t < 20 h,
320 Figure 2) along with the removal of nitrate (Figure S2) indicated that sulfur-driven
321 autotrophic denitrification may occur in CWs. In order to validate this hypothesis,
322 autotrophic denitrification kinetic tests were carried out. Table 1 shows that without
323 organic matter, the autotrophic denitrification rates ranged from 34.7–50.7 mg N m^{-2} d^{-1}
324 in litter-added CWs, and this accounted for 7%–16% of the total nitrate removal. The
325 remaining proportion was removed by heterotrophic denitrification and plant uptake.
326 Furthermore, the simultaneous formation of sulfate was observed in the litter-added
327 CWs, and the observed sulfide oxidation rates ($r_{SO\text{-}O}$) were very close to the expected
328 theoretical sulfide oxidation rates ($r_{SO\text{-}T}$), according to Eq. (1) (Table 1). This suggested
329 that S-driven autotrophic denitrification occured in litter-added CWs and this is
330 represented by Eq. (1) below.

331 $$55S^0 + 50NO_3^- + 38H_2O + 20CO_2 + 4NH_4^+ \longrightarrow 4C_5H_7O_2N + 55SO_4^{2-} + 25N_2 + 64H^+ \quad (1)$$

332 **3.5 Microbial communities related to S cycling**

333 Microbial community analyses were carried out for the gravel and litter in the

wetland microcosms at the end of the experiment. A total of 30884 high-quality sequence tags were obtained from the biofilms in the unplanted (W_0), litter-added (W_1), and planted (W_3) microcosms. Figure S4 shows that both SRB and SOB were found in the W_0 and W_1 microcosms. However, both types of bacteria were below the detection limit of the Roche 454 high-throughput pyrosequencer in the W_3 microcosm. *Desulfobacter*, *Desulfovibrio*, *Desulfobulbus*, *Desulfococcus* and *Desulfocapsa* were the dominant SRB genera (1.1%-9.3%), whereas *Sulfuricurvum* and *Thiobacillus* were the dominant SOB genera (1.5%-6.1%). Furthermore, uncultured species dominated SRB diversity in the microcosms. Interestingly, the relative abundances of SRB and SOB were higher in litter than in gravel. This indicated that the litter could act as a good biofilm carrier for the S-related microbes, and suggested that on-site S transformation may occur in the plant litter.

4. Discussion

4.1 Sulfate transformation in CWs

Sulfate is an electron acceptor commonly found in water and wastewater. In assimilatory sulfate reduction (ASR), sulfate can be integrated into organic S via uptake by plants and/or microorganisms. In dissimilatory sulfate reduction (DSR), sulfate is reduced to sulfide after the transfer of eight electrons. A previous study have shown that ASR contributed less than 0.3% to sulfate removal in wetlands, which means that DSR is probably the dominant pathway for sulfate removal (Wu et al., 2013). In this study,

ACCEPTED MANUSCRIPT

354 the presence of cattail (*Typha latifolia*) made no significant contribution to sulfate
355 reduction (Figure 2), which was consistent with the results from a previous study (Chen
356 et al., 2014a). The low sulfate removal in the planted microcosms was probably due to
357 root-mediated oxygen transfer, which would increase the redox potential and decrease
358 the SRB activity (Stein et al., 2007). In contrast to the plants, adding cattail litter greatly
359 stimulated the sulfate reduction due to the continuous input of labile organic carbon.
360 However, the sulfate removal rates gradually decreased in the litter-added microcosms.
361 The high sulfate removal rates during the initial stage were probably due to the rapid
362 leaching of carbon sources (e.g. sugars) in the litter; and the low sulfate removal rates
363 during the terminal stage were probably caused by the slow decomposition of
364 recalcitrant materials (e.g. lignin) (Chimney and Pietro, 2006).

365 Despite the various sulfate removal rates observed in the microcosms, the sulfide
366 concentrations were always low, and were much smaller than the theoretical sulfide
367 production through sulfate reduction. In this study, the accumulation of solid AVS in the
368 gravel indicated that the produced sulfide could have escaped from the water via metal
369 sulfide precipitation. Additionally, S^0 formation (Figure 3) and increased sulfate
370 concentration ($t < 20$ h, Figure 2) in the microcosms suggested that sulfide re-oxidation
371 may have occurred. Previous studies found that 41%–90% of the reduced S was
372 re-oxidized by root-mediated oxygen in planted wetlands (Wiessner et al., 2010; Wu et
373 al., 2011). In this study, the nitrate in the influent was another electron acceptor that

ACCEPTED MANUSCRIPT

374 could drive sulfide oxidation to sulfate in CWs (Section 3.4).

375 In wetlands, S^0 can be produced via either chemical or microbial oxidation of
376 sulfide, or be eliminated through oxidation to sulfate or by bacterial disproportionation
377 (Wu et al., 2011). Thus, S^0 is an important intermediate product in the wetland S cycle.
378 Figure 3 shows that the S^0 concentrations were not stable during the initial and middle
379 stages and this was probably caused by further oxidation to sulfate when sulfide is
380 limited. The S^0 concentrations reached a steady state during the terminal stage, and
381 there was a balance between S^0 formation and consumption. In DSR, the sulfate is
382 firstly activated to form adenosine phosphosulfate (APS) and then APS is reduced to
383 form sulfite. After this, sulfite can be directly reduced to sulfide or indirectly reduced to
384 sulfide with the formation of thiosulfate (Ren et al., 2009). In this study, thiosulfate was
385 only observed in the litter-added microcosms and its concentration rose as the carbon
386 sources levels increased. Wiessner et al. (2010) also found that thiosulfate can
387 accumulate in wetlands when there was a high carbon loading. The absence of
388 thiosulfate under the carbon limited condition was probably due to the preferential
389 utilization of a reduction pathway that allows SRB to obtain a higher energy yield when
390 the electron donor is limited (Ren et al., 2009). In addition, some factors (e.g.
391 temperature and pH) have also been reported to influence thiosulfate generation and
392 accumulation (Qian et al., 2015).

393 Solid AVS was the most abundant S compound in the litter-added microcosms, and

accounted for 65.4%–77.0% of total sulfate removal (Figure 5). This suggested that a major proportion of the sulfide was precipitated along with metals and accumulated on the gravel after sulfate reduction. The AVS method (cold 1 N HCl) used in this study cannot quantitatively extract mackinawite, greigite and pyrite S (Rickard and Morse, 2005). This means that the AVS contents were probably underestimated. However, the disadvantages of this method do not affect the conclusions of this study. A previous study also found that most of the sulfate was converted to AVS in a wetland sediment with an S loading similar to this study (Baldwin and Mitchell, 2012). In this study, Fe oxides/oxyhydroxides are the dominant ferric mineral in the gravels. The reducing conditions in CWs should cause the reductive dissolution of Fe-oxys and thereby release ferric ion, indicating an important ferrous source for the formation of AVS. The intense S (-II) peak (Figure 4) and abundant Fe (4.7%, Figure S3) on the gravel surface further demonstrated the existence of Fe-S precipitation (FeS_2) in the litter-added microcosms. Pyrite (FeS_2) is widely considered to be a primary source of AVS in riverine, lake, and wetland sediments, and it can be oxidized via chemical and microbial pathways (Burton et al., 2009; Johnston et al., 2014; Zeng et al., 2013). In this study, the limited oxygen concentration in the influent and the long-term flooding operation created low redox conditions in the microcosms (–200 ~ 50 mV), which may have decreased the pyrite oxidation rates (Johnston et al., 2014). Furthermore, the organic carbon released by the litter could also compete with the reduced S for oxygen, thereby

414 slowing pyrite oxidation (Rigby et al., 2006). In addition to pyrite, some metastable iron
415 sulfides (e.g. mackinawite and greigite) may also be present in the gravel surface layer
416 and play a role in S cycling. Further studies need to produce quantitative descriptions of
417 reactive Fe speciation.

418 **4.2 Sulfur cycling pathways and the roles of microorganisms**

419 Cattail is an aquatic plant that is widely used in CWs. During the decomposition of
420 plant litters, lignocelluloses are first hydrolyzed by extracellular hydrolytic enzymes and
421 then fermented into the liable carbon sources that drive sulfate reduction (Zhao et al.,
422 2009). Bacterial sulfate reduction carried out by SRB is widely considered to be the
423 dominant process involved in sulfate removal from CWs due to the significant
424 enrichment of the heavier ^{34}S isotope (Wu et al., 2011). A previous study reported that
425 SRB was usually divided into non-acetate oxidizers and acetate oxidizers (Hansen,
426 1993). The non-acetate oxidizers (*Desulfobulbus, Desulfovibrio and Desulfobacterium*)
427 could utilize the liable fermentation products (hydrogen, lactate and pyruvate) as
428 electron donors, and thus reduce sulfate to sulfide. The acetate oxidizers (*Desulfobacter*,
429 *Desulfococcus* and *Desulfosarcina*) could oxidize acetate to CO_2 via TCA or acetyl-CoA
430 pathways (Ren et al., 2009). Previous studies have also suggested that *Desulfobacter*,
431 *Desulfovibrio*, *Desulfobulbus*, *Desulfococcus* and *Desulfobacterium* are the
432 representative SRBs in wetlands (King et al., 2002; Lloyd et al., 2004; Russell et al.,
433 2003). In this study, numerous different SRBs were found in the litter-added

ACCEPTED MANUSCRIPT

434 microcosms. Among them, *Desulfobacter* and *Desulfovibrio* were very abundant in the
435 litter-added microcosms (Figure S4), which indicated that the SRB could reduce sulfate
436 using either acetate or other fermentation products as electron donors. The reduction in
437 carbon sources produced during litter decomposition suggested that the SRB would
438 compete with other microorganisms (e.g. methanogens) for available organic carbon
439 (e.g. acetate), which could strongly influence the sulfate reduction rates during long
440 operation of wetlands (Chen et al., 2014a).

441 After sulfate reduction, reduced S was produced and most of the sulfide was
442 precipitated with Fe to form AVS on the gravel (Figure 5). Previous studies showed that
443 the metal sulfide may be permanently immobilized in the sediments of wetlands if there
444 is an anaerobic environment in the beds (Johnston et al., 2014; Wu et al., 2013).
445 However, in this study, both oxygen and nitrate were present in the influent, which
446 suggests that reduced S would become oxidized by chemical or microbial pathways. A
447 previous study revealed that S microbial oxidation was much faster than chemical
448 oxidation, and both aerobic oxidation (using oxygen as electron acceptor) and anoxic
449 oxidation (using nitrate as electron acceptor) could contribute to the microbial oxidation
450 of sulfide (Plas et al., 1992). If oxygen is unlimited, then a majority of the S would be
451 oxidized by aerobic oxidation. However, the influent oxygen concentration was limited
452 (< 1 mg L^{-1}), and oxygen transport rate from air to water was very low (k_{La} = 0.1 d^{-1}) in
453 this study. The theoretical calculation indicated that the oxygen from the influent flow

ACCEPTED MANUSCRIPT

454 and air transfer could only oxidize 1–1.5 mg L^{-1} S to sulfate, much lower than the
455 sulfate production in the litter-added microcosms (Figure 2). This suggested that anoxic
456 microbial oxidation of sulfide to sulfate could be another pathway in the wetland S
457 cycle. The mediation of sulfide oxidation by SOB has been reported by several groups
458 (*Acidithiobacillus*, *Chromatium* and *Beggiatoa*) (Holmer and Storkholm, 2001). In this
459 study, the SOBs, *Thiobacillus thioparus* and *Sulfuricurvum kujiense*, were abundant in
460 the litter-added microcosms. They can use nitrate to oxidize sulfide, and couple the
461 denitrification to S oxidation (Read-Daily et al., 2011). In this study, an increase in
462 sulfate ($t < 20$ h, Figure 2) was concurrent with a decrease in nitrate (Figure S2). This
463 indicated that they have roles in both S oxidation and nitrate reduction. The matched
464 autotrophic denitrification rates (r_{AD}) and the sulfide oxidation rates ($r_{SO\text{-}O}$) further
465 support this idea (Table 1). Additionally, the presence of *Desulfobulbus/Desulfocapsa*
466 suggested that disproportionate S^0 to sulfide/sulfate was possible to occur in CWs when
467 sulfide concentrations were low (Finster et al., 1998; Lovley and Phillips, 1994).

468 **4.3 Implications for tertiary wastewater treatment**

469 In this study, the plant litter was reused as a self-supplying carbon source for
470 sulfate reduction, and iron-rich gravel was used to efficiently immobilize the produced
471 sulfide. This cooperation optimizes the carbon flow in wetlands and buffers sulfide
472 toxicity in the receiving water body. Most significantly, simultaneous sulfur-driven
473 autotrophic (S^0 or AVS as the electron donor) and heterotrophic denitrification (litter
474 carbon as the electron donor) can be achieved in one CW. When the influent nitrate

loading rates are low and carbon sources are sufficient for complete heterotrophic denitrification, the residual carbon sources will drive sulfate reduction and transfer the electron to sulfur (S^0 or AVS). Furthermore, S-driven autotrophic denitrification can occur during periods of high nitrate loading when heterotrophic denitrification alone is not sufficient to remove nitrate. Therefore, this study provides a promising, low-cost technology for tertiary or decentralized wastewater treatment when nitrogen loading rates are highly variable. Furthermore, S-based mixotrophic denitrification would greatly reduce the demand for organic carbon and wetland area compared to full heterotrophic denitrification. Although a litter-added CW with iron-rich filling material is an efficient ecosystem for sulfur and nitrogen removal, the benefits of iron-rich filling material must also be weighed against potential drawbacks. It has been reported that phosphate and sulfide removal efficiency declined in CWs with iron-rich gravel due to competition and iron exhaustion (Wu et al., 2012). Hence, further research is needed to investigate the dynamics of S, phosphate, and ferrous interactions during the long-term operation of CWs.

5. Conclusions

In this study, S transformations were investigated in CWs with and/or without plant. The results showed that the presence of *Typha latifolia* had a marginal effect on sulfate removal, but its carbon-rich litter greatly promoted sulfate removal. After sulfate reduction, most of the produced sulfide was immobilized on the iron-rich gravel surface

ACCEPTED MANUSCRIPT

with only minor amounts lost through oxidation. Acid volatile sulfide and two valence states, S (-II) and S (0), were identified in the precipitate attached to the gravel surface. Elemental S and thiosulfate were detected as the intermediates in the pore water. Sulfur species quantification further showed that AVS was the main sink for the transformed sulfate-S (65%–77%), and elemental S and other unknown S compounds accounted for 5%–8% and 10%–26%, respectively. Most significantly, results showed that S-driven mixotrophic denitrification in CWs could effectively remove nitrate along with sulfide oxidation, which may lead to the simultaneous removal of organics, nitrate, and sulfate without excess toxic sulfide output during tertiary wastewater treatment.

Acknowledgments

This work was financially supported by the National Science Foundation of China (51578393), the Fundamental Research Funds for the Central Universities (20113139), and the Czech University of Life Sciences and ESF & MEYS (CZ.1.07/2.3.00/30.0040).

Appendix A. Supplementary material

Supplementary data associated with this article are available in the online version.

References

APHA, 1998. Standard Methods for the Examination of Water and Wastewater, 20th ed, American Public Health Association ed. American Public Health Association, Washington, DC, USA.

Baldwin, D.S., Mitchell, A., 2012. Impact of sulfate pollution on anaerobic biogeochemical cycles in a wetland sediment. Water Research, 46, 965-974.

Burton, E.D., Bush, R.T., Sullivan, L.A., Hocking, R.K., Mitchell, D.R.G., Johnston, S.G.,

516 Fitzpatrick, R.W., Raven, M., McClure, S., Jang, L.Y., 2009. Iron-monosulfide oxidation in
517 natural sediments: Resolving microbially mediated S transformations using xanes, electron
518 microscopy, and selective extractions. Environmental Science and Technology, 43, 3128-3134.
519 Chen, Y., Wen, Y., Cheng, J., Xue, C.H., Yang, D.H., Zhou, Q., 2011. Effects of dissolved oxygen on
520 extracellular enzymes activities and transformation of carbon sources from plant biomass:
521 Implications for denitrification in constructed wetlands. Bioresource Technology, 102,
522 2433-2440.
523 Chen, Y., Wen, Y., Tang, Z.R., Huang, J.G., Zhou, Q., Vymazal J., 2015. Effects of plant biomass on
524 bacterial community structure in constructed wetlands used for tertiary wastewater treatment.
525 Ecological Engineering, 84, 38-45.
526 Chen, Y., Wen, Y., Zhou, J., Tang, Z., Li, L., Zhou, Q., Vymazal, J., 2014a. Effects of cattail biomass
527 on sulfate removal and carbon sources competition in subsurface-flow constructed wetlands
528 treating secondary effluent. Water Research, 59, 1-10.
529 Chen, Y., Wen, Y., Zhou, Q., Vymazal, J., 2014b. Effects of plant biomass on nitrogen transformation
530 in subsurface-batch constructed wetlands: A stable isotope and mass balance assessment. Water
531 Research, 63, 158-167.
532 Chimney, M.J., Pietro, K.C., 2006. Decomposition of macrophyte litter in a subtropical constructed
533 wetland in south Florida (USA). Ecological Engineering, 27, 301-321.
534 Crist, B.V., 1999. Handbook of Monochromatic XPS Spectra: Vol.1—The Elements and Native
535 Oxides. XPS International, California.
536 EPA, U., 2004. Guidelines for Water Reuse. U.S. Environmental Protection Agency, Report No.
537 EPA/625/R-04/108, Cincinnati, Ohio, USA.
538 Faulwetter, J.L., Gagnon, V., Sundberg, C., Chazarenc, F., Burr, M.D., Brisson, J., Camper, A.K.,
539 Stein, O.R., 2009. Microbial processes influencing performance of treatment wetlands: A
540 review. Ecological Engineering, 35, 987-1004.
541 Finster, K., Liesack, W., Thamdrup, B., 1998. Elemental sulfur and thiosulfate disproportionation by
542 Desulfocapsa sulfoexigens sp nov, a new anaerobic bacterium isolated from marine surface

543 sediment. Applied and Environmental Microbiology, 64, 119-125.
544 Greenway, M., 2004. The role of constructed wetlands in secondary effluent treatment and water
545 reuse in subtropical and and Australia. 87th Canadian Chemistry Conference and Exhibition,
546 London, CANADA, pp. 501-509.
547 Hallberg, K.B., Johnson, D.B., 2005. Microbiology of a wetland ecosystem constructed to remediate
548 mine drainage from a heavy metal mine. Science of The Total Environment, 338, 53-66.
549 Hansen, A., 1993. Carbon metabolism of sulfate-reducing bacteria. in: Odom, J.M., Rivers-Singleton,
550 J.R. (Eds.). The Sulfate-Reducing Bacteria: Contemporary Perspectives. Springer-Verlag, New
551 York, pp. 21-40.
552 Holmer, M., Storkholm, P., 2001. Sulphate reduction and sulphur cycling in lake sediments: a review.
553 Freshwater Biology, 46, 431-451.
554 Hume, N.P., Fleming, M.S., Horne, A.J., 2002. Denitrification potential and carbon quality of four
555 aquatic plants in wetland microcosms. Soil Science Society of America Journal, 66, 1706-1712.
556 Jasper, J.T., Jones, Z.L., Sharp, J.O., Sedlak, D.L., 2014. Biotransformation of trace organic
557 contaminants in open-water unit process treatment wetlands. Environmental Science and
558 Technology, 48, 5136-5144.
559 Johnston, S.G., Burton, E.D., Aaso, T., Tuckerman, G., 2014. Sulfur, iron and carbon cycling
560 following hydrological restoration of acidic freshwater wetlands. Chemical Geology, 371, 9-26.
561 King, J.K., Harmon, S.M., Fu, T.T., Gladden, J.B., 2002. Mercury removal, methylmercury
562 formation, and sulfate-reducing bacteria profiles in wetland mesocosms. Chemosphere, 46,
563 859-870.
564 Krishnakumar, B., Manilal, V.B., 1999. Bacterial oxidation of sulphide under denitrifying conditions.
565 Biotechnology Letters, 21, 437-440.
566 Lloyd, J.R., Klessa, D.A., Parry, D.L., Buck, P., Brown, N.L., 2004. Stimulation of microbial
567 sulphate reduction in a constructed wetland: microbiological and geochemical analysis. Water
568 Research, 38, 1822-1830.
569 Londry, K.L., Suflita, J.M., 1999. Use of nitrate to control sulfide generation by sulfate-reducing

570 bacteria associated with oily waste. Journal of Industrial Microbiology & Biotechnology, 22,
571 582-589.
572 Lovley, D.R., Phillips, E.J.P., 1994. Novel Processes for anaerobic sulfate production from elemental
573 sulfur by sulfate-reducing bacteria. Applied and Environmental Microbiology, 60, 2394-2399.
574 Margulies, M., Egholm, M., Altman, W.E., Attiya, S., Bader, J.S., Bemben, L.A., Berka, J.,
575 Braverman, M.S., Chen, Y.J., Chen, Z.T., Dewell, S.B., Du, L., Fierro, J.M., Gomes, X.V.,
576 Godwin, B.C., He, W., Helgesen, S., Ho, C.H., Irzyk, G.P., Jando, S.C., Alenquer, M.L.I., Jarvie,
577 T.P., Jirage, K.B., Kim, J.B., Knight, J.R., Lanza, J.R., Leamon, J.H., Lefkowitz, S.M., Lei, M.,
578 Li, J., Lohman, K.L., Lu, H., Makhijani, V.B., McDade, K.E., McKenna, M.P., Myers, E.W.,
579 Nickerson, E., Nobile, J.R., Plant, R., Puc, B.P., Ronan, M.T., Roth, G.T., Sarkis, G.J., Simons,
580 J.F., Simpson, J.W., Srinivasan, M., Tartaro, K.R., Tomasz, A., Vogt, K.A., Volkmer, G.A.,
581 Wang, S.H., Wang, Y., Weiner, M.P., Yu, P.G., Begley, R.F., Rothberg, J.M., 2005. Genome
582 sequencing in microfabricated high-density picolitre reactors. Nature, 437, 376-380.
583 Nicomrat, D., Dick, W.A., Tuovinen, O.H., 2006. Assessment of the microbial community in a
584 constructed wetland that receives acid coal mine drainage. Microbial Ecology, 51, 83-89.
585 Plas, C., Harant, H., Danner, H., Jelinek, E., Wimmer, K., Holubar, P., Braun, R., 1992. Ratio of
586 biological and chemical oxidation during the aerobic elimination of sulfide by colorless sulfur
587 bacteria. Applied Microbiology and Biotechnology, 36, 817-822.
588 Qian, J., Lu, H., Cui, Y., Wei, L., Liu, R., Chen, G.H., 2015. Investigation on thiosulfate-involved
589 organics and nitrogen removal by a sulfur cycle-based biological wastewater treatment process.
590 Water Research, 69, 295-306.
591 Read-Daily, B., Tank, J., Nerenberg, R., 2011. Stimulating denitrification in a stream mesocosm with
592 elemental sulfur as an electron donor. Ecological Engineering, 37, 580-588.
593 Ren, N.Q., Wang, A.J., Zhao, Y.G., 2009. Ecology of Sulfate-Reducing Bacteria in Anaerobic
594 Biotreatment Processes. Sciencep, China.
595 Rickard, D., Morse, J.W., 2005. Acid volatile sulfide (AVS). Marine Chemistry, 97, 141-197.
596 Rigby, P.A., Dobos, S.K., Cook, F.J., Goonetilleke, A., 2006. Role of organic matter in framboidal

597 pyrite oxidation. Science of The Total Environment, 367, 847-854.
598 Russell, R.A., Holden, P.J., Wilde, K.L., Neilan, B.A., 2003. Demonstration of the use of
599 Scenedesmus and Carteria biomass to drive bacterial sulfate reduction by Desulfovibrio
600 alcoholovorans isolated from an artificial wetland. Hydrometallurgy, 71, 227-234.
601 Stein, O.R., Borden-Stewart, D.J., Hook, P.B., Jones, W.L., 2007. Seasonal influence on sulfate
602 reduction and zinc sequestration in subsurface treatment wetlands. Water Research, 41,
603 3440-3448.
604 Sun, M., Mu, Z.X., Chen, Y.P., Sheng, G.P., Liu, X.W., Chen, Y.Z., Zhao, Y., Wang, H.L., Yu, H.Q.,
605 Wei, L., Ma, F., 2009. Microbe-assisted sulfide oxidation in the anode of a microbial fuel cell.
606 Environmental Science and Technology, 43, 3372-3377.
607 Wen, Y., Chen, Y., Zheng, N., Yang, D.H., Zhou, Q., 2010. Effects of plant biomass on nitrate
608 removal and transformation of carbon sources in subsurface-flow constructed wetlands.
609 Bioresource Technology, 101, 7286-7292.
610 Wiessner, A., Rahman, K.Z., Kuschk, P., Kastner, M., Jechorek, M., 2010. Dynamics of sulphur
611 compounds in horizontal sub-surface flow laboratory-scale constructed wetlands treating
612 artificial sewage. Water Research, 44, 6175-6185.
613 Wu, S.B., Chen, Z.B., Braeckevelt, M., Seeger, E.M., Dong, R.J., Kastner, M., Paschke, H., Hahn, A.,
614 Kayser, G., Kuschk, P., 2012. Dynamics of Fe(II), sulphur and phosphate in pilot-scale
615 constructed wetlands treating a sulphate-rich chlorinated hydrocarbon contaminated
616 groundwater. Water Research, 46, 1923-1932.
617 Wu, S.B., Kuschk, P., Wiessner, A., Muller, J., Saad, R.A.B., Dong, R.J., 2013. Sulphur
618 transformations in constructed wetlands for wastewater treatment: A review. Ecological
619 Engineering, 52, 278-289.
620 Wu, S.B.A., Jeschke, C., Dong, R.J., Paschke, H., Kuschk, P., Knoller, K., 2011. Sulfur
621 transformations in pilot-scale constructed wetland treating high sulfate-containing contaminated
622 groundwater: A stable isotope assessment. Water Research, 45, 6688-6698.
623 Zeng, T., Arnold, W.A., Toner, B.M., 2013. Microscale characterization of sulfur speciation in lake

sediments. Environmental Science and Technology, 47, 1287-1296.

Zhao, B.H., Yue, Z.B., Ni, B.J., Mu, Y., Yu, H.Q., Harada, H., 2009. Modeling anaerobic digestion of aquatic plants by rumen cultures: Cattail as an example. Water Research, 43, 2047-2055.

Table caption

Table 1. Reaction rates for nitrate removal (r_{NR}), autotrophic denitrification (r_{AD}) and sulfide oxidation (r_{SO}) in five wetland microcosms.

Figure captions

Figure 1. The schematic diagram of experimental design concept of this study.

Figure 2. Sulfate and sulfide concentrations in the different wetland microcosms during the initial stage (a, batch 4), middle stage (b, batch 12) and terminal stage (c, batch 20).

Figure 3. Elemental S and thiosulfate S concentrations in the W0–W4 microcosms during the initial stage (a) batch 4, middle stage (b) batch 12, and terminal stage (c) batch 20.

Figure 4. Evolution of XPS S2*p* spectra for the substances on gravel surface in the W1, W2 and W4 microcosms.

Figure 5. Distribution of S species in litter-added wetland microcosms based on the S mass balance calculation.

ACCEPTED MANUSCRIPT

Table 1 — Reaction rates for nitrate removal (r_{NR}), autotrophic denitrification (r_{AD}) and sulfide oxidation (r_{SO}) in five wetland microcosms.

	r_{NR} [a] mg-N m^{-2} d^{-1}	r_{AD} [b] mg-N m^{-2} d^{-1}	r_{SO-O} [c] mg-S m^{-2} d^{-1}	r_{SO-T} [d] mg-S m^{-2} d^{-1}
W0	44.4	8.0	nd.	20.1
W1	269.6	42.7	104.0	107.3
W2	611.0	50.7	114.7	127.4
W3	208.1	10.7	nd.	26.8
W4	491.8	34.7	93.3	87.2

a r_{NR}, nitrate removal rates, were obtained from the nitrate removal kinetic in batch 20.

b r_{AD}, autotrophic denitrification rates, were obtained from the variations of nitrate concentrations in the autotrophic denitrification kinetic tests (without organic matter).

c r_{SO-O}, observed sulfide oxidation rates, were obtained from the variations of sulfate concentrations in the autotrophic denitrification kinetic tests.

d r_{SO-T}, theoretical sulfide oxidation rates, were obtained from the theoretical calculations of sulfate formation for a complete sulfur-based autotrophic denitrification.

nd. not detectable.

ACCEPTED MANUSCRIPT

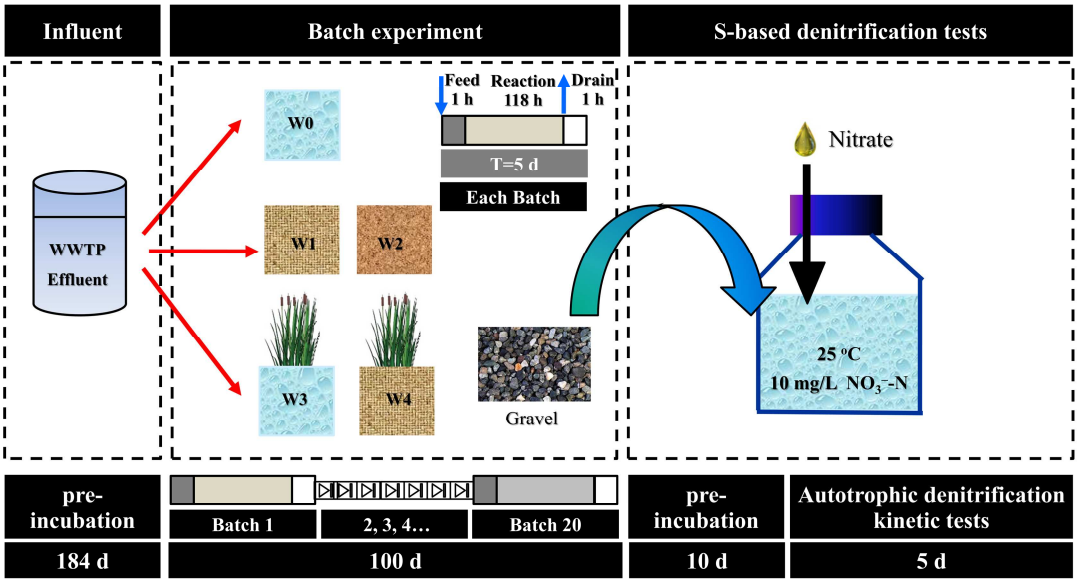

Figure 1 The schematic diagram of experimental design concept of this study.

ACCEPTED MANUSCRIPT

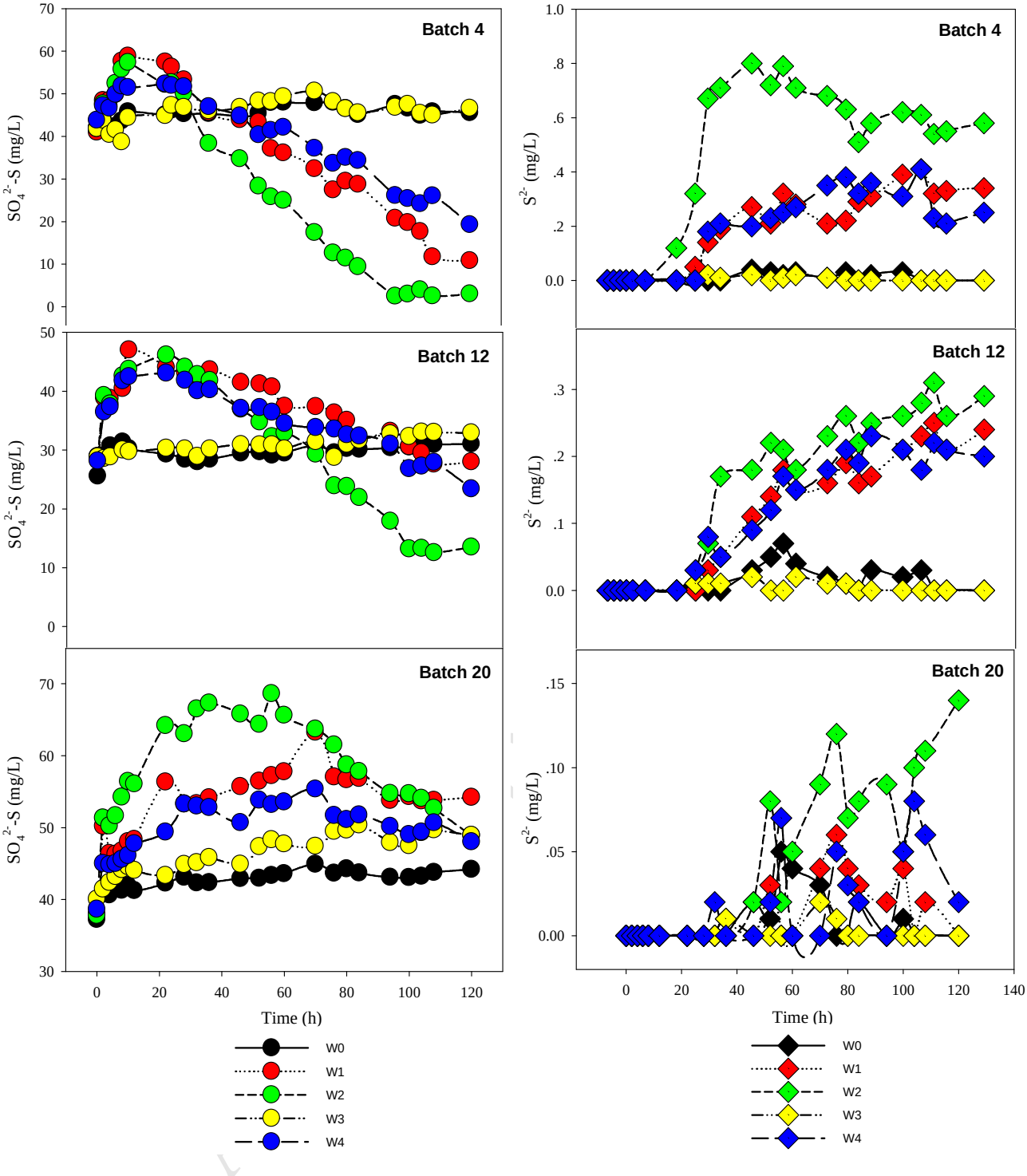

Figure 2 Sulfate and sulfide concentrations in the different wetland microcosms during the initial stage (a, batch 4), middle stage (b, batch 12) and terminal stage (c, batch 20).

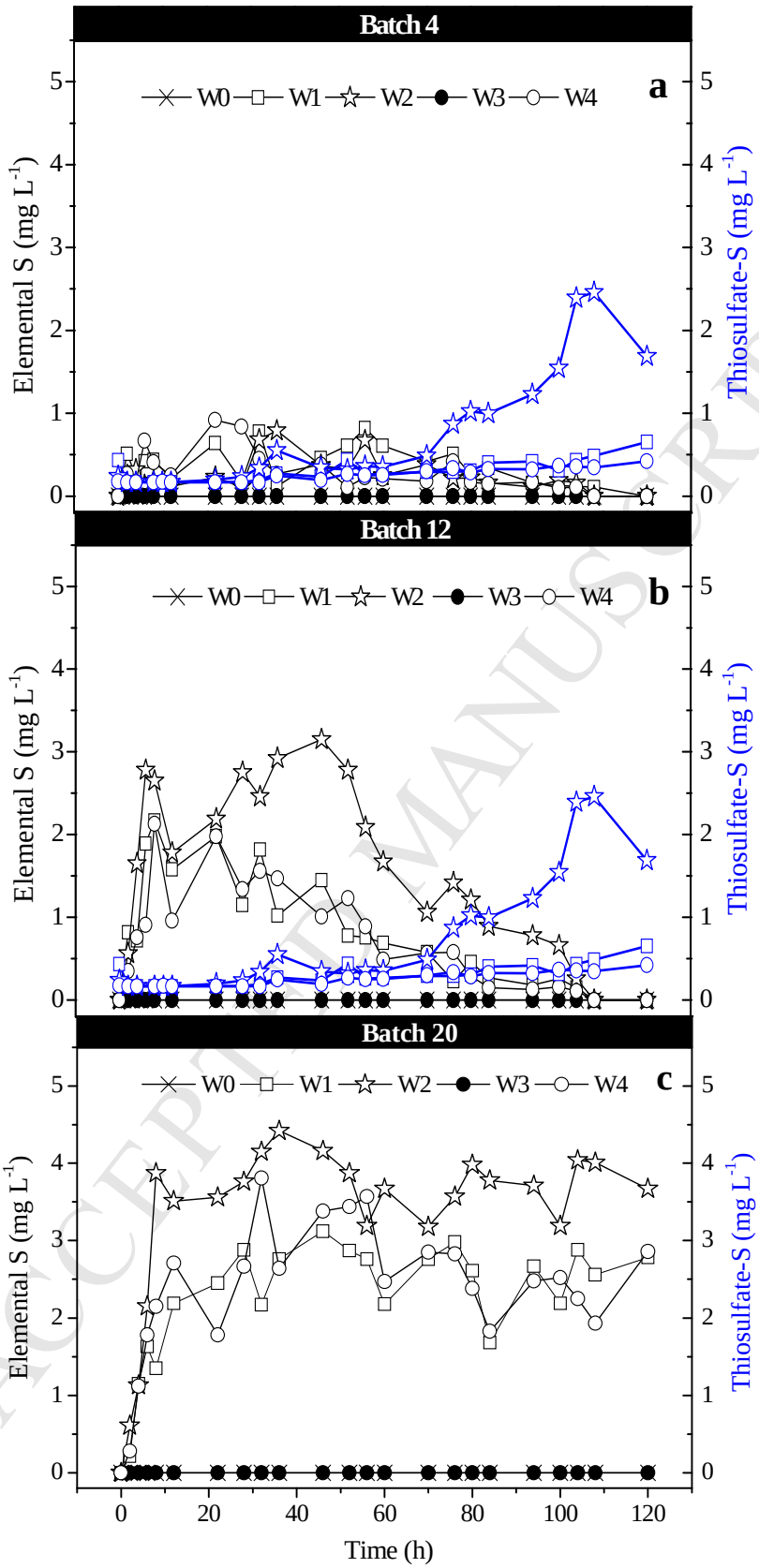

Figure 3. Elemental S and thiosulfate S concentrations in the W0–W4 microcosms during the initial stage (a) batch 4, middle stage (b) batch 12, and terminal stage (c) batch 20.

ACCEPTED MANUSCRIPT

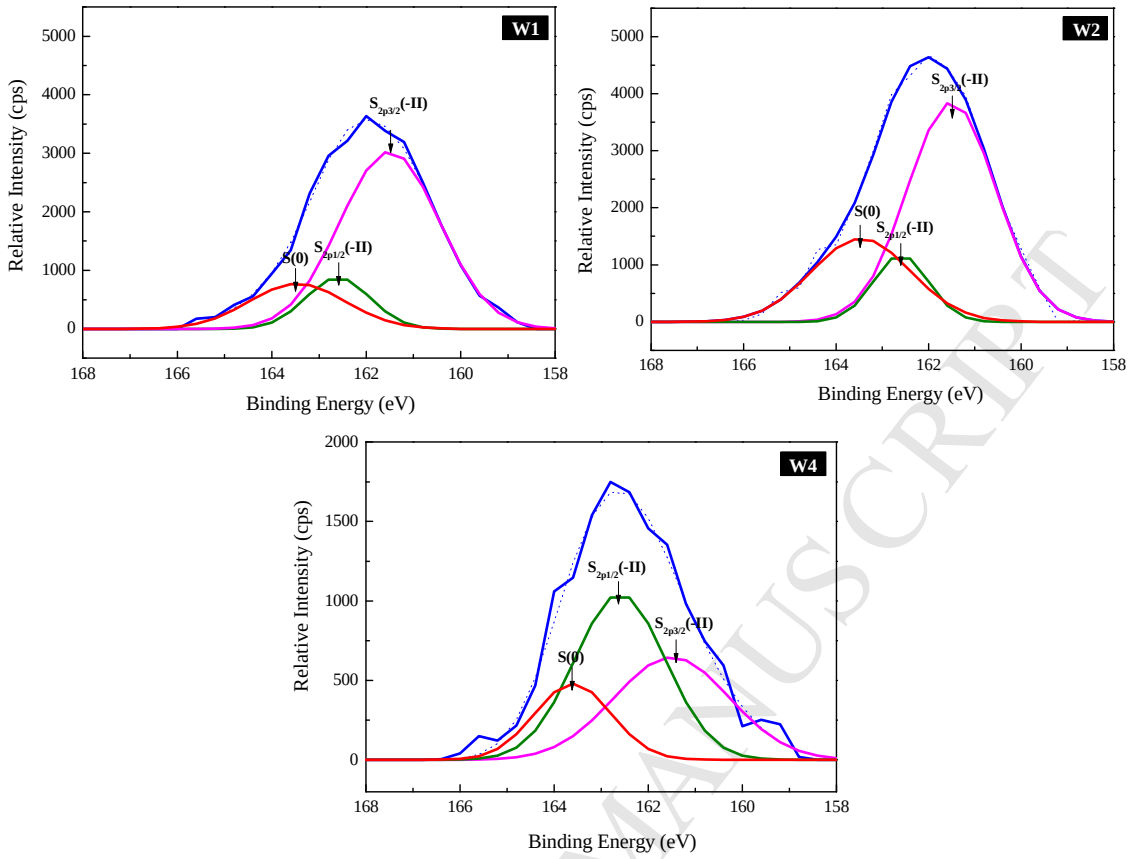

Figure 4 Evolution of XPS S2*p* spectra for the substances on gravel surface in the W1, W2 and W4 microcosms.

ACCEPTED MANUSCRIPT

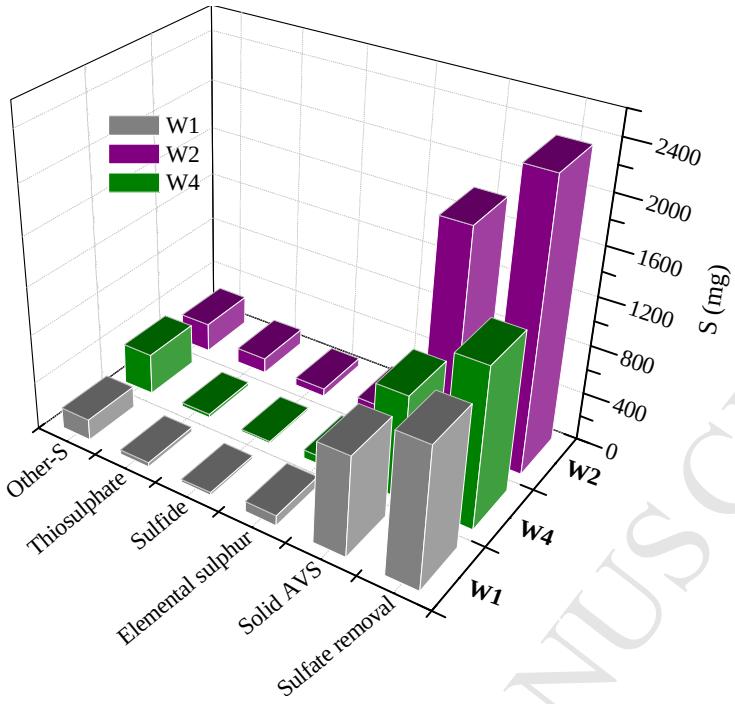

Figure 5 Distribution of S species in litter-added wetland microcosms based on the S mass balance calculation.

ACCEPTED MANUSCRIPT

ACCEPTED MANUSCRIPT

Highlights

- Sulfur transformation processes in CWs were characterized.
- Simultaneous removal of sulfate without excess sulfide output was achieved.
- The transformed sulfate-S was mainly immobilized as acid volatile sulfide.
- The sulfide can be re-oxidized to elemental sulfur and sulfate in CWs.
- Sulfur-driven mixotrophic denitrification occurs in CWs.

ACCEPTED MANUSCRIPT